Simultaneous Global Identification of Dynamic and Network Parameters in Transient Stability Studies

Mark K. Transtrum, Benjamin L. Francis
Dept. of Physics and Astronomy
Brigham Young University, UT, USA
mktranstrum@byu.edu

Andrija T. Sarić [1], Aleksandar M. Stanković [2]
[1] Dept. of Power, Electronics and Com. Engineering
[1] University of Novi Sad, Faculty of Technical Sciences, Serbia
[2] Dept. of Electrical and Computer Engineering
[2] Tufts University, Medford, MA, USA
[1] asaric@uns.ac.rs; [2] astankov@ece.tufts.edu

***Abstract*—The paper describes a global identification procedure for dynamic power system models in the form of differential and algebraic equations. Power system models have a number of features that makes their improvement challenging – they are multi-level, multi-user and multi-physics. Not surprisingly, they are nonlinear and time varying, both in terms of states (memory variables) and parameters, and discrete structures, such as graphs, are strongly blended with continuous dynamics, resulting in network dynamics. The transient stability models are used as a prototypical example. Our method is based on information geometry, and uses advances in computational differential geometry to characterize high-dimensional manifolds in the space of measurements. In the case of network parameters, a comparison is presented with circuit-theoretic techniques. The results are illustrated on the case of IEEE 14-bus test system with 58 parameters in our realization.**

***Index Terms*— System Identification, Global Optimization, Parameter Estimation.**

I. Introduction

Models used in studies of dynamic phenomena in power systems such as transient stability have significantly advanced in terms of size and level of detail. At the same time, they do encounter difficulties when trying to replicate well-documented events from actual power systems [1]. Given the changes in power systems involving markets, distributed sources and agglomerated loads (such as microgrids), it is likely that the challenges will persist well into the future.

One natural approach is then to try to improve models using operational data. Indeed, the system identification concept has been used in power systems for decades, mostly in the form of model tuning for key components, such as synchronous generators [2]. However, system identification is not without its own challenges, mostly related to possibly local nature and suboptimality of a solution, to over-parametrization of models for typical measurement structures, and to multi-scale nature of power systems, as evidenced by differential-algebraic equations (DAE) used to describe their dynamics. The concept is, however, helped by the emergence of new measurement devices, such as Phasor Measurement Units, and of new parameter estimation procedures.

In this paper we explore the capabilities of information geometry to perform identification of a networked system. The procedure combines information theory and differential geometry. Its foundation is the interpretation of a model as a manifold embedded in the space of data, known as the model manifold. Information geometry captures the global properties of the model, since the manifold retains information about all model predictions [3]. In contrast, the cost surface in parameter space condenses the high-dimensional quantities, such as the prediction and measurement vectors into a single number – the cost. We have quantified the information-geometric properties of some power system components in [4-6]; here we look at properties of a networked system with 58 unknown parameters and consider network reduction and partial response matching.

In the sequel we briefly review only the references with direct connections to our considerations. The term network dynamics is used in [7] to describe systems in which discrete structures, such as graphs are blended with dynamical relationships describing components connected in nodes. The identifiability of linear dynamic networks with known topology is discussed in [8]. The case of static radial networks with unknown topology and parameters is addressed in [9]. In this work authors assume known network topology, and study global identifiability properties of nonlinear DAE models.

The outline of the paper is as follows: in *Section II* is provided the problem formulation; *Section III* describes the Manifold Boundary Approximation Method (MBAM); *Section IV* shows the optimization formulation of the network reduction sub-problem; proposed method is applied to the benchmark 14-bus system in *Section V*, and *Section VI* presents conclusions.

II. Problem Formulation

The standard DAE form of power system models used in transient stability is [10]:

$$\dot{\boldsymbol{x}} = \boldsymbol{f}(\boldsymbol{x}, \boldsymbol{z}, \boldsymbol{p}, t)\,, \tag{1}$$

$$\boldsymbol{0} = \boldsymbol{g}(\boldsymbol{x}, \boldsymbol{z}, \boldsymbol{p}, t)\,, \tag{2}$$

where $\boldsymbol{x}$ is the vector of (differential) state variables, $\boldsymbol{z}$ are the algebraic variables, $\boldsymbol{p}$ are parameters (typically assumed to be unknown in estimation studies) and t is the (scalar) time variable. System measurement vector is assumed to be of the form:

$$\boldsymbol{y} = \boldsymbol{h}(\boldsymbol{x}, \boldsymbol{z}, \boldsymbol{p}, t)\,. \tag{3}$$

The parameters ($\boldsymbol{p}$) are to be estimated from measurements ($\boldsymbol{y}$); there typically exists prior information about individual parameters, often in the form of plausible ranges for each. The

978-1-5386-7703-2/18/$31.00 ©2018 IEEE

key quantities are parametric sensitivities whose dynamics is described by the following equations:

$$\frac{\partial \dot{\boldsymbol{x}}}{\partial \boldsymbol{p}} = \frac{\partial \boldsymbol{f}(\boldsymbol{x},\boldsymbol{z},\boldsymbol{p},t)}{\partial \boldsymbol{x}} \cdot \frac{\partial \boldsymbol{x}}{\partial \boldsymbol{p}} + \frac{\partial \boldsymbol{f}(\boldsymbol{x},\boldsymbol{z},\boldsymbol{p},t)}{\partial \boldsymbol{z}} \cdot \frac{\partial \boldsymbol{z}}{\partial \boldsymbol{p}} + \frac{\partial \boldsymbol{f}(\boldsymbol{x},\boldsymbol{z},\boldsymbol{p},t)}{\partial \boldsymbol{p}}; \quad (4)$$

$$\boldsymbol{0} = \frac{\partial \boldsymbol{g}(\boldsymbol{x},\boldsymbol{z},\boldsymbol{p},t)}{\partial \boldsymbol{x}} \cdot \frac{\partial \boldsymbol{x}}{\partial \boldsymbol{p}} + \frac{\partial \boldsymbol{g}(\boldsymbol{x},\boldsymbol{z},\boldsymbol{p},t)}{\partial \boldsymbol{z}} \cdot \frac{\partial \boldsymbol{z}}{\partial \boldsymbol{p}} + \frac{\partial \boldsymbol{g}(\boldsymbol{x},\boldsymbol{z},\boldsymbol{p},t)}{\partial \boldsymbol{p}}; \quad (5)$$

$$\frac{\partial \boldsymbol{h}}{\partial \boldsymbol{p}} = \frac{\partial \boldsymbol{h}(\boldsymbol{x},\boldsymbol{z},\boldsymbol{p},t)}{\partial \boldsymbol{x}} \cdot \frac{\partial \boldsymbol{x}}{\partial \boldsymbol{p}} + \frac{\partial \boldsymbol{h}(\boldsymbol{x},\boldsymbol{z},\boldsymbol{p},t)}{\partial \boldsymbol{z}} \cdot \frac{\partial \boldsymbol{z}}{\partial \boldsymbol{p}} + \frac{\partial \boldsymbol{h}(\boldsymbol{x},\boldsymbol{z},\boldsymbol{p},t)}{\partial \boldsymbol{p}}. \quad (6)$$

These equations are linear in terms of sensitivities, but the matrices involved vary along each system trajectory.

III. Manifold Boundary Approximation Method (MBAM)

Inferring all the parameters of a large, complicated model is often difficult [3]. The reason for this difficulty is the insensitivity of the model's predictions to coordinated changes in the values of its parameters. This insensitivity suggests a simpler model can describe the same set of observations. We use the Manifold Boundary Approximation Method (MBAM) to remove the unidentifiable combinations of parameters from the model. MBAM was first applied to power systems in [5]. Briefly, MBAM leverages a geometric interpretation of statistics. In this approach, the model is a manifold with parameters as coordinates. The key insight leveraged by MBAM is that typical model manifolds are bounded. The boundary has a hierarchical structure similar to a polygon. That is, the manifold is bounded by several faces that meet at edges, corners, etc. Each of these boundary cells corresponds to a simplifying approximation to the model. Using computational differential geometry, we identify the appropriate boundary cell that captures most of the model's predictive power.

Following the methods described in [5], we find boundary cells by solving the geodesic equation on the model manifold. Along geodesics, some parameters are pushed to extreme values (zero or infinity). By evaluating the limit that some parameters become infinity or zero, we construct simplified models with fewer parameters. For example, the geodesic may push the time constant for subtransients to zero, leading to a singular perturbation approximation of the model. After a new model has been constructed, we identify its parameter values by fitting them to the predictions of the original model. The entire process is iterated, removing one parameter at a time, until all parameters are constrained by the available measurements, i.e., further reductions can no longer match the predictions of the original model.

IV. Formulation of Classical Network Reduction

In the MBAM model reduction procedure, the susceptance of a transmission line connecting two nodes eventually becomes the parameter whose value takes one of the two extreme values (disconnecting the line or shortening the two nodes involved). This network changes can also be analyzed from a network-theory perspective, and in this section we compare the results of the two procedures. To set the network-theoretic counterpart of the MBAM line removal (as we haven't encountered in our examples the insertion of a short between two nodes), we start with basic bus power balance equations:

$$\underline{\boldsymbol{I}} = \underline{\boldsymbol{Y}}_{bus}\underline{\boldsymbol{V}}, \text{ or } \underline{\boldsymbol{V}} = \underline{\boldsymbol{Z}}_{bus}\underline{\boldsymbol{I}}; \quad (7)$$

$$\underline{\boldsymbol{S}} = diag(\underline{\boldsymbol{V}})\underline{\boldsymbol{I}}^{*} = diag(\underline{\boldsymbol{V}})\underline{\boldsymbol{Y}}_{bus}^{*}\underline{\boldsymbol{V}}^{*}, \quad (8)$$

where:

$\underline{\boldsymbol{I}}$ – N_{bus}-dimensional vector of bus complex current injections;

$\underline{\boldsymbol{V}}$ – N_{bus}-dimensional vector of bus complex voltages;

$\underline{\boldsymbol{S}}$ – N_{bus}-dimensional vector of bus complex power injections;

$\underline{\boldsymbol{Y}}_{bus} = \boldsymbol{E}^{\mathrm{T}}\underline{\boldsymbol{Y}}^{b}\boldsymbol{E}$ – (N_{bus}×N_{bus})-dimensional bus admittance matrix;

$\underline{\boldsymbol{Z}}_{bus} = \underline{\boldsymbol{Y}}_{bus}^{-1}$ – bus impedance matrix;

$\boldsymbol{E}$ – (N_b×N_{bus})-dimensional branch-bus incidence matrix, with elements ±1 for ending buses of the branch;

$\underline{\boldsymbol{Y}}^{b}$ – N_b-dimensional diagonal branch admittance matrix, with elements $\underline{Y}_l^b = 1/\underline{Z}_l^b$, where $\underline{Z}_l^b$ is impedance of l–th branch;

N_{bus}, N_b – number of system buses and branches, respectively.

After l–th branch opening (between buses m and n), a new bus admittance matrix is

$$\underline{\boldsymbol{Y}}_{bus}^{(1)} = \underline{\boldsymbol{Y}}_{bus}^{(0)} + \underline{Y}_l^b \boldsymbol{e}_l \boldsymbol{e}_l^{\mathrm{T}}, \quad (9)$$

where $\boldsymbol{e}_l$ is N_{bus}-dimensional branch-bus incidence vector, with elements +1 on m–th and −1 on n–th position.

The MBAM procedure optimizes over $\underline{Y}_l^b$ (remaining after branch removal) and other model parameters to match the measurements via non-linear least squares. Here we consider a simpler, but related problem – we assume (nearly) constant current injections in nodes before/after branch removal and we optimize over bus admittance matrices with known structure. It turns out that this results in linear least squares (LLS) problem. It may be tempting to simply try to match the original admittance matrix over matrices with restricted structure (without a given line), but this formulation misses the directional properties of nodal matrices that are key in matching the line flows.

When $\underline{\boldsymbol{I}}$ assumed nearly the same ($\underline{\boldsymbol{I}} = \underline{\boldsymbol{I}}^{(1)} = \underline{\boldsymbol{I}}^{(0)}$), $\underline{\boldsymbol{V}}$ should also change little ($\underline{\boldsymbol{V}} \approx \underline{\boldsymbol{V}}^{(0)} \approx \underline{\boldsymbol{V}}^{(1)}$)

$$\underline{\boldsymbol{I}} = \underline{\boldsymbol{Y}}_{bus}^{(1)}\underline{\boldsymbol{V}} \approx \underline{\boldsymbol{Y}}_{bus}^{(1)}\underline{\boldsymbol{Z}}_{bus}^{(0)}\underline{\boldsymbol{I}}. \quad (10)$$

Please note that this assumption may turn out to be only partially true in practice. The network reduction procedure may, however, still produce a useful list of candidate branches for model reduction, as we show below. An alternative optimization-based procedure is offered by the MBAM procedure, and we compare the two methods in the next *Section*.

Thus the specified optimization problem becomes

$$min \left\| \underline{\boldsymbol{Y}}_{bus}^{(1),opt}\underline{\boldsymbol{Z}}_{bus}^{(0)} - \boldsymbol{1} \right\|, \quad (11)$$

or

$$\min_{\underline{\boldsymbol{Y}}^{b(1),opt}} \left\| \left(\boldsymbol{E}^{(1)}\right)^{\mathrm{T}} \underline{\boldsymbol{Y}}^{b(1),opt} \boldsymbol{E}^{(1)} \underline{\boldsymbol{Z}}_{bus}^{(0)} - \boldsymbol{1} \right\|, \quad (12)$$

where $\boldsymbol{1}$ is appropriately sized identity matrix.

Optimization problem (12) can be solved by using its structure

$$\boldsymbol{AXB} = \boldsymbol{C}, \quad (13)$$

yield

$$(\boldsymbol{B}^{\mathrm{T}} \otimes \boldsymbol{A}) vec(\boldsymbol{X}) = vec(\boldsymbol{C}), \quad (14)$$

where $\boldsymbol{X} \equiv \underline{\boldsymbol{Y}}^{b(1),opt}$ with additional constraints to decision variables for $i \neq j$

$$X_{ij} = 0, \quad (15)$$

and where $\otimes$ denotes Kronecker product, $vec(\cdot)$ is vectorized matrix, $\boldsymbol{A} \equiv \left(\boldsymbol{E}^{(1)}\right)^{\mathrm{T}}$ and $\boldsymbol{B} \equiv \boldsymbol{E}^{(1)}\underline{\boldsymbol{Z}}_{bus}^{(0)}$ [11].

Since the decision vector $\boldsymbol{X}$ is diagonal, the optimization problem (12) can be rearranged to $m = 1, 2, \ldots, N_{bus} \cdot N_{bus}$ linear complex equations as

$$\sum_{k=1}^{N_b} A_{ik} \underline{B}_{kj} \underline{X}_k = b_m;$$
$$i, j = 1, 2, \ldots, N_{bus};\ k = 1, 2, \ldots, N_{br}^{(1)}, \qquad (16)$$

where $b_m = \begin{cases} 1, & i = j \\ 0, & i \neq j \end{cases}$.

Optimization problem (12) can be written in linear complex form as

$$\min_{\underline{x}} \left\| \underline{\boldsymbol{A}} \underline{\boldsymbol{x}} - \boldsymbol{b} \right\|, \qquad (17)$$

where the LLS optimal solution is

$$\underline{\boldsymbol{x}} = \underline{\boldsymbol{A}}^{\mathrm{T}} (\underline{\boldsymbol{A}}\, \underline{\boldsymbol{A}}^{\mathrm{T}})^{-1} \boldsymbol{b}. \qquad (18)$$

V. Application

A. Test system

IEEE 14-bus model used here includes five synchronous generators in Buses 1, 2, 3, 6, and 8, Figure 1. The generator in Bus 1 is implemented as a fourth-order model, including rotor angle, speed, and transient electromotive forces in the d- and q-axes. The generators in Buses 2 and 3 are implemented as a classical, second-order model for the generator speed and rotor angle. The generators in Buses 6 and 8 are both modeled as a detailed, sixth-order model, including both transient and subtransient dynamics in the d- and q-axes. We assume many parameters, such the moments of inertia for rotors, are not to be estimated from transient dynamics and fixed to predetermined values. This setup, aimed at exploring networked system aspects, leads to a model with 38 tunable component parameters describing both generator and some controller elements.

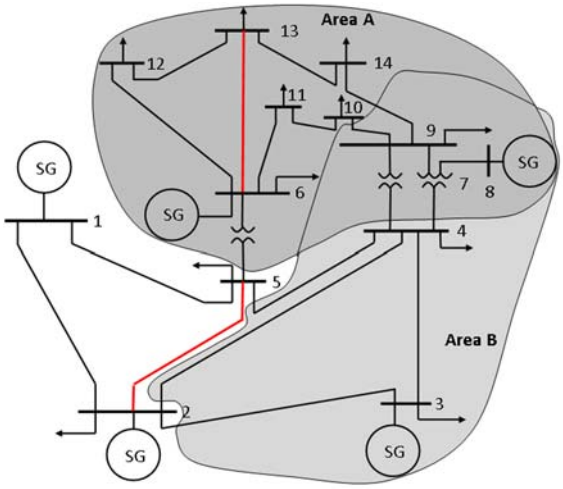

Figure 1. 14-bus test system with reduced branches

B. System-Wide Identification

For each network edge we take the susceptance as a tunable parameter. We model the conductance as being proportional to the susceptance on each edge, giving a total of 20 network parameters. The entire model has 58 parameters.

We assume the system is initially in steady state, that it is perturbed at $t = 0$, and that the subsequent transient is observed. We introduce this transient by increasing the mechanical power seen by each generator. We consider here the case of measurements (or local estimates [4]) of the generators' rotor angle, speed, and real and reactive powers. We also assume voltage magnitude and angle are available in each bus. Typical transients at generator are shown in Figures 2 and 3 for generators in Buses 2 and 6, respectively. We discuss dependence of our results on these details in the next section.

Notice the mismatch in the reactive power (middle right panel) in Figure 3 which indicates that the reduced model is identifiable, but the match is not perfect.

We conducted a sensitivity analysis by numerically solving the sensitivity (4)-(6) and calculating the Fisher Information Matrix (FIM). We show the eigenvalues of the FIM for this model in Figure 4, column a. Notice that the eigenvalues of this matrix are uniformly spaced in log over almost 8 orders of magnitude, indicating much more sensitivity of the model's predictions to variations in some combinations of parameters than in others.

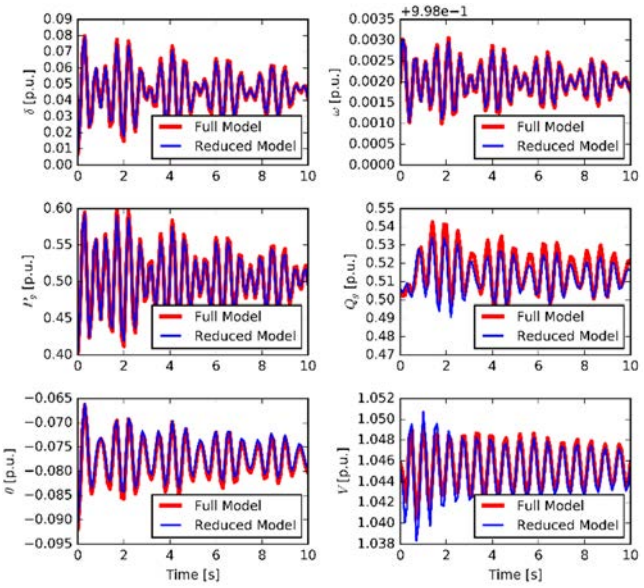

Figure 2. Transients to be matched in Bus 2 before (red) and after (blue) model reduction, including rotor angle, frequency, real and reactive power of the generator and angle and voltage in the bus. The reduced model still has good agreement with the full model.

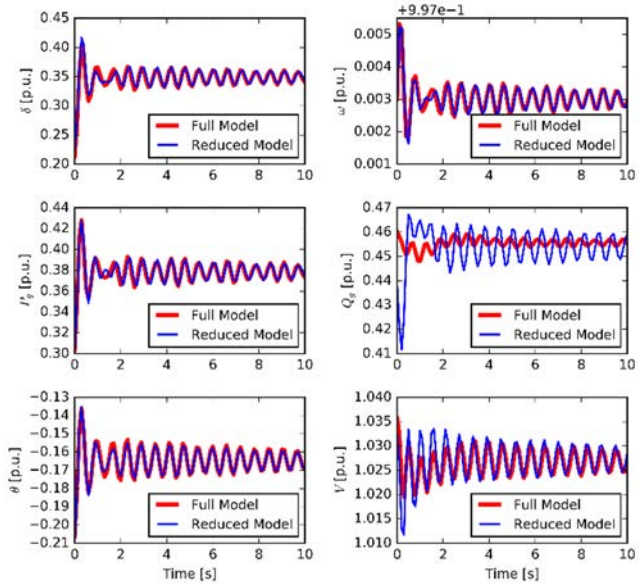

Figure 3. Transients to be matched in Bus 6. Mismatch in the reactive power (middle right panel) indicates that all parameters are identifiable from these observations.

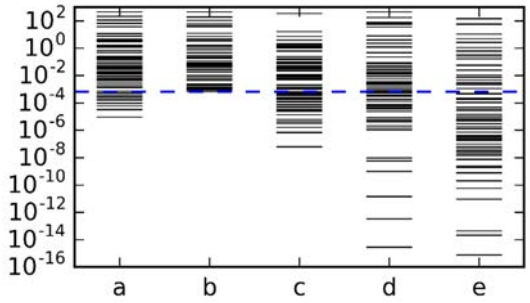

Figure 4. Eigenvalue spectra of the FIM, showing (a) the full model with all observations, (b) the reduced model with all observations, (c) the full model, observing only area A, (d) the full model, observing only power and voltage in generators and generator buses, and (e) the full model, observing only Buses 1 and 14 (buyer/seller relationship). The dashed line marks the smallest eigenvalue of the reduced model. Additional reduction could be achieved by observing only part of the system.

Using MBAM, we are able to reduce the 58-parameter model down to one with 45 parameters. The parameter values along a typical geodesic curve are shown in Figure 5. Further reductions are possible in principle, but we find these models do not faithfully reproduce the all of transients of the 58-parameter model, as we discuss below. The sequence of limiting approximations that reduces the number of parameters to 45 is shown in Table I.

We find that the 45-parameter model is able to accurately match the transient behavior for all the model predictions, except for the reactive power in Bus 6. We show the transients of the 45-parameter model for the generators in two buses in Figures 1 and 2. In Bus 2, the match is still quite good, but in Bus 6 there are visible deviations, most notably for reactive power, but also for the voltage. From this we conclude that further reductions of the model would significantly reduce its accuracy for this set of predictions. We discuss the potential for further simplifications relative to other predictions in *Section V.C*.

We conduct a FIM-based sensitivity analysis of the 45-parameter model. Eigenvalues of this reduced model are shown in Figure 4, column b. Notice that MBAM has succeeded in removing the least identifiable parameters in the model. Indeed, by comparing with column a we see that the effect of MBAM has been to "erase" the 12 smallest eigenvalues, leaving untouched the parameters most important for determining the model's behavior.

It is interesting to consider the specific sequence of approximations identified by MBAM. Most of the approximations are

TABLE I. REDUCTION STEPS.

Step	Number of parameters	Reduced parameter	Reduced element	Type
1	57	$x''_d \to x'_d$	Bus 6	
2	56	$T''_{d0} \to 0$	Bus 6	Singular Limit
3	55	$B_{2,5} \to 0$	Line 2-5	Network Reduction
4	54	$x''_q \to x'_q$	Bus 8	
5	53	$T''_{q0} \to 0$	Bus 8	Singular Limit
6	52	$x''_q \to x'_q$	Bus 6	
7	51	$T''_{q0} \to 0$	Bus 6	Singular Limit
8	50	$x'_d \to x_d$	Bus 1	
9	49	$B_{6,13} \to 0$	Line 6-13	Network Reduction
10	48	$x''_d \to x'_d$	Bus 8	
11	47	$T''_{d0} \to 0$	Bus 8	Singular Limit
12	46	$x'_d \to x_d$	Bus 6	
13	45	$T'_{d0} \to 0$	Bus 6	Singular Limit

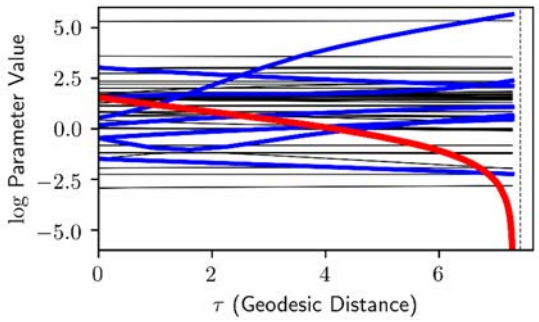

Figure 5. Parameter values along a geodesic in step 2. Here, $T''_{d0} \to 0$ in Bus 6 (i.e., its log value goes to negative infinity in red) corresponding to a singular perturbation that removes the *d*-axis subtransient. In order to compensate for this approximation, several other parameter values change (blue lines), while most other parameter values are constant (black curves).

singular perturbations. Each of these is paired with a limit in which a subtransient reactance is removed. Nominally, MBAM removes one parameter from the model at a time. Since singular perturbation in the subtransients also removes the reactances, this processes is a two-step procedure in the MBAM.

It is perhaps unsurprising that MBAM identifies a series of singular limits for the simplification of model components. What is less intuitive, however, is the network reduction in steps 3 and 8. Here, MBAM has identified 2 branches that can be effectively removed from the model without altering model predictions. We analyze these predictions in *Section V.C*.

C. Partial Response Matching

The MBAM procedure is a data-driven model reduction procedure in the sense that it identifies and removes parameters from a model that would be unidentifiable for a given set of observations. Consequently, the results of *Section V.B* are conditional on the choice of observation function. Both theoretical and numerical studies have demonstrated that the results of MBAM are robust to certain changes in observations. For example, using tools of differential topology it can be shown that MBAM selected models are robust to things, such as the number of time points [12]. In contrast, changing which variables are observed can lead to different reduced models. In this section we consider how the results of *Section V.B* depend on the choice of observation function.

We conduct a sensitivity analysis of the 14-bus model in which only a subset of the observations is considered. The eigenvalues of the FIM are show in Figure 4 for several alternative choices of observations. First, we restrict the observations to those in **Area A** in Figure 1, i.e., Buses 6–14. Because these measurements carry less information than those in *Section V.B*, the FIM eigenvalues decrease (column c in Figure 4), indicating that fewer parameters can be identified and more parameters could be removed by MBAM. Next, we consider the case in which we observe only the power and voltages in buses with generators (column d in Figure 4). Finally, we consider a very sparse choice of observations in which we only variables in Buses 1 and 14 (column e), suggestive of a designated buyer/seller relationship.

Using the results of *Section V.B*, we can estimate how many parameters a minimal model we require for each of the observation functions in Figure 4. Recall that each iteration of MBAM effectively removes the smallest FIM eigenvalue from the model. Thus, the value of the smallest eigenvalue of the 45-

parameter model (column b) sets the scale at which parameters can be effectively identified from data (dashed line in Figure 4). The number of eigenvalues larger than this is the approximate number of parameters that would be retained by MBAM. We estimate that the **Area A** measurements (column c) could be fit by 38 parameters. Observing only power and voltages (column d) could be fit by about 35 parameters, while the buyer/seller model (column e) could be fit by about 20 parameters.

D. Comparison of MBAM and Classical Network Reduction

When the MBAM procedure is applied to the IEEE 14-bus system, it disconnects branch 2-5 at step 3, and branch 6-13 at step 8 (see Figure 1). We compare these results with the network reduction in Tables II and III. Table II suggests that the network optimized as in (12) leads to reasonable results that match the network flows and losses very well. Table III displays that the parameter tuning has a physically reasonable both in MBAM and in (12). For example, line 2-5 removal increases susceptance in nearby branch 1-5. The same can be noticed for retuned line 6-12 following the removal of 6-13. Note that these two methods rank candidate branches for removal; at the next step, the optimization of (remaining) parameters determines the quality of the proposed system simplification, and possibly rejects it.

TABLE II. POWER FLOW RESULTS.

	Basic case						Branch 2-5 removed						Branches 2-5 and 6-13 removed					
Bus	V_i	θ_i	Load		Generation		V_i	θ_i	Load		Generation		V_i	θ_i	Load		Generation	
	[p.u.]	[rad]	[MW]	[MVAr]	[MW]	[MVAr]	[p.u.]	[rad]	[MW]	[MVAr]	[MW]	[MVAr]	[p.u.]	[rad]	[MW]	[MVAr]	[MW]	[MVAr]
1	1.060	0.000	0.000	0.000	2.387	–0.181	1.060	0.000	0.000	0.000	2.383	–0.155	1.060	0.000	0.000	0.000	2.410	–0.154
2	1.045	–0.092	0.304	0.178	0.400	0.537	1.045	–0.092	0.304	0.178	0.400	0.492	1.045	–0.097	0.304	0.178	0.400	0.548
3	1.010	–0.258	1.319	0.266	0.000	0.487	1.010	–0.253	1.319	0.266	0.000	0.490	1.010	–0.263	1.319	0.266	0.000	0.518
4	1.023	–0.173	0.669	0.056	0.000	0.000	1.024	–0.159	0.669	0.056	0.000	0.000	1.020	–0.171	0.669	0.056	0.000	0.000
5	1.031	–0.148	0.106	0.022	0.000	0.000	1.031	–0.134	0.106	0.022	0.000	0.000	1.027	–0.146	0.106	0.022	0.000	0.000
6	1.070	–0.216	0.157	0.105	0.300	0.619	1.070	–0.203	0.157	0.105	0.300	0.611	1.070	–0.221	0.157	0.105	0.300	0.549
7	1.035	–0.148	0.000	0.000	0.000	0.000	1.036	–0.136	0.000	0.000	0.000	0.000	1.029	–0.155	0.000	0.000	0.000	0.000
8	1.090	–0.039	0.000	0.000	0.700	0.379	1.090	–0.028	0.000	0.000	0.700	0.379	1.090	–0.046	0.000	0.000	0.700	0.428
9	1.013	–0.209	0.413	0.232	0.000	0.000	1.013	–0.196	0.413	0.232	0.000	0.000	1.000	–0.221	0.413	0.232	0.000	0.000
10	1.013	–0.217	0.126	0.081	0.000	0.000	1.013	–0.204	0.126	0.081	0.000	0.000	1.001	–0.228	0.126	0.081	0.000	0.000
11	1.036	–0.219	0.049	0.025	0.000	0.000	1.036	–0.207	0.049	0.025	0.000	0.000	1.028	–0.227	0.049	0.025	0.000	0.000
12	1.046	–0.236	0.085	0.022	0.000	0.000	1.046	–0.224	0.085	0.022	0.000	0.000	1.014	–0.261	0.085	0.022	0.000	0.000
13	1.037	–0.236	0.189	0.081	0.000	0.000	1.037	–0.223	0.189	0.081	0.000	0.000	0.952	–0.281	0.189	0.081	0.000	0.000
14	0.997	–0.247	0.209	0.070	0.000	0.000	0.998	–0.234	0.209	0.070	0.000	0.000	0.952	–0.274	0.209	0.070	0.000	0.000
Total			3.626	1.140	3.787	1.841			3.626	1.140	3.783	1.819			3.626	1.140	3.810	1.888
Losses			0.161	0.701					0.157	0.679							0.183	0.748

TABLE III. BRANCH IMPEDANCES.

Branch	Basic case	Branch 2-5 removed	Branches 2-5 and 6-13 removed
2–5	0.05695+j0.17390	∞	∞
6–12	0.12290+j0.25580	0.12290+j0.35095	0.12290+j0.25185
12–13	0.22090+j0.19990	0.22090+j0.19503	0.22090+j0.21533
6–13	0.06615+j0.13030	0.06615+j0.15819	∞
6–11	0.09498+j0.19890	0.09498+j0.22225	0.09498+j0.23330
10–11	0.08205+j0.19210	0.08205+j0.19456	0.08205+j0.19461
9–10	0.03181+j0.08450	0.03181+j0.09000	0.03181+j0.08999
9–14	0.12710+j0.27040	0.12710+j0.29045	0.12710+j0.32536
13–14	0.17090+j0.34800	0.17090+j0.33426	0.17090+j0.33768
7–9	0.00000+j0.11000	0.00000+j0.10906	0.00000+j0.10911
1–2	0.01938+j0.05917	0.01938+j0.06493	0.01938+j0.06285
2–3	0.04699+j0.19800	0.01938+j0.18747	0.01938+j0.18620
3–4	0.06701+j0.17100	0.06701+j0.20776	0.06701+j0.20845
1–5	0.05403+j0.22300	0.05403+j0.20509	0.05403+j0.23399
4–5	0.01335+j0.04211	0.01335+j0.04635	0.01335+j0.04657
2–4	0.05811+j0.17630	0.05811+j0.20663	0.05811+j0.20510
5–6	0.00000+j0.25200	0.00000+j0.43418	0.00000+j0.55129
4–9	0.00000+j0.55620	0.00000+j1.02606	0.00000+j1.02496
4–7	0.00000+j0.20910	0.00000+j0.25007	0.00000+j0.25005
7–8	0.00000+j0.17620	0.00000+j0.18695	0.00000+j0.18696

VI. CONCLUSION

In this paper we describe a global system identification procedure (MBAM) that simultaneously reduces the dynamic model, and estimates network and component parameters. We also present a circuit-theoretic interpretation of the network reduction sub-problem. It turns out that MBAM and the circuit-based procedure are largely aligned, providing an engineering insight into a high-dimensional optimization problem. Our ongoing efforts focus on scaling-up the procedure via computational improvements and network decomposition, and on applications to larger benchmark power systems.

REFERENCES

[1] Andersson, G., et al.: "Causes of the 2003 major grid blackouts in North America and Europe, and recommended means to improve system dynamic performance", IEEE Trans. Power Syst., 2005, **20** (4), pp. 1922–1928.

[2] Burth, M., Verghese, G.C., Velez-Reyes M.: "Subset selection for improved parameter estimation in on-line identification of a synchronous generator", IEEE Trans. Power Syst., 1999, **14** (1), pp. 218–225.

[3] Transtrum, M.K., Machta, B.B., Sethna, J.P.: "Why are nonlinear fits to data so challenging?", Physical Review Letters, 2010, **104** (1), pp. 1–4.

[4] Transtrum, M.K., Sarić, A.T., Stanković, A.M.: "Information geometry approach to verification of dynamic models in power systems", IEEE Trans. Power Syst., 2018, **33** (1), pp. 440–450.

[5] Transtrum, M.K., Sarić, A.T., Stanković, A.M.: "Measurement-directed reduction of dynamic models in power systems", IEEE Trans. Power Syst., 2017, **32** (3), pp. 2243–2253.

[6] Sarić, A.T., Transtrum, M.K., Stanković, A.M.: "Information geometry for model identification and parameter estimation in renewable energy – DFIG plant case", IET Generation, Transmission and Distribution, 2018, accepted for publication, **DOI:** 10.1049/iet-gtd.2017.0606

[7] van der Schaft, A.J., Maschke, B.M.: "Port Hamiltonian systems on graphs", SIAM J. Control Optimization, 2013, **51** (2), pp. 906–937.

[8] Bazanella, A.S., Gevers, M., Hendrickx, J.M., Parraga, A.:, "Identifiability of dynamical networks: which nodes need be measured", arXiv:1709.04398v1, 2017.

[9] Yu, J., Weng, Y., Rajagopal, R.: "PaToPa: a data driven parameter and topology joint estimation framework in distribution grids", arXiv:1705.08870v1, 2017.

[10] Kundur, P.: *Power System Stability and Control*, McGraw-Hill, 1994.

[11] Hou, J., Peng, Z.Y., Zhang, X.: "An iterative method for the least squares symmetric solution of matrix equation $AXB = C$", Numer. Algor., 2006, **42** (2), pp. 181–192.

[12] Transtrum, M.K., Hart, G.L.W., Qiu, P.: "Information topology identifies emergent model classes", arXiv:1409.6203v2, 2016.